Relationship among O, Mg isotopes and the petrography of two spinel-bearing compound chondrules

SEIJI MARUYAMA[1,*] and HISAYOSHI YURIMOTO[2]

[1]Institute for Study of the Earth's Interior, Okayama University, Yamada 827, Misasa, Tohaku, Tottori 682-0193, Japan
[2]Earth and Planetary Sciences, Tokyo Institute of Technology, Meguro, Tokyo 152-8551, Japan

Abstract—The petrological properties, and O and Al-Mg isotopic compositions of two spinel-bearing chondrules from the Allende CV chondrite were investigated using scanning electron microscopy and secondary ion mass spectrometry. A coarse spinel grain in a barred-olivine (BO) chondrule is less enriched in ^{16}O ($\Delta^{17}O \sim -5‰$; $\Delta^{17}O = \delta^{17}O - 0.52 \; \delta^{18}O$), whereas smaller spinel grains in a plagioclase-rich chondrule member of a compound chondrule are extremely ^{16}O-rich ($\Delta^{17}O \sim -17‰$) and the spinels have a strongly serrated character. The petrological features and ^{16}O-enrichments of the spinels in the plagioclase-rich chondrule indicate that spinels originating in coarse-grained Ca-Al-rich Inclusions (CAIs) were incorporated into chondrule precursors and survived the chondrule-forming event. The degree of ^{16}O-excesses among minerals within each chondrule is correlated to the crystallization sequences. This evidence suggests that the O isotopic variation among minerals may have resulted from incomplete exchange of O isotopes between ^{16}O-rich chondrule melt and ^{16}O-poor nebular gas. Aqueous alteration also has changed the O-isotope compositions in the mesostasis. The feldspathic mesostasis in the BO chondrule shows a disturbed Mg-Al isochron indicating that the BO chondrule experienced secondary alteration. While plagioclase in the plagioclase-rich chondrule member of the compound chondrule shows slight ^{26}Mg-excesses corresponding to $(^{26}Al/^{27}Al)_0 = [4.6 \pm 4.0(2\sigma)] \times 10^{-6}$, nepheline formed by secondary alteration shows no detectable excess. The Al-Mg isotopic system of these chondrules was disturbed by aqueous alteration and thermal metamorphism on the Allende parent body. *Copyright © 2003 Elsevier Ltd*

1. INTRODUCTION

Two of the primary constituents of chondritic meteorites, namely Ca-Al-rich Inclusion (CAIs) and chondrules contain important clues to the understanding of early solar system processes and history. Chondrules are believed to have formed from clumps of precursor dust by transient heating events (e.g., Grossman, 1988). CAIs probably formed by high temperature processes in the solar nebula, such as volatilization, recondensation, and melting. CAIs have larger ^{16}O-excesses and larger quantities of short-lived nuclides such as ^{26}Al than chondrules (Clayton, 1993; Russell et al., 1996). These facts indicate the common conclusion that chondrules and CAIs formed by different processes, at times (e.g., Russell et al., 1996) and/or places far removed from one another (e.g., Wood, 1996a, 1996b).

Chondrules and CAIs could have formed compound objects among the same constituents (Rubin, 1994). Two or more chondrules combined as compound chondrules are sometimes observed. The earlier view of the formation of compound chondrules is the "random-collision-while-molten" model (Gooding and Keil, 1981; Lux et al., 1981) which calls for two independently formed chondrules to collide while one or both was/were still molten. A more recent interpretation view is the "relict-chondrule" model (Wasson, 1993; Wasson et al., 1995); it calls for the primary chondrule to be part of a porous precursor assemblage that was flash heated and melted to form the secondary chondrule.

Compound CAIs are also observed. The compound CAIs recognized by Wark and Lovering (1982) are composite Type B1-in-Type A CAIs separated by palisades (chains of spinel crystals). Wark and Lovering (1982) argued that some large Type B1 bodies might have served as nuclei around which Type A grains aggregated and to which they became welded by continuing condensation or by secondary alteration processes. Isotopic evidence regarding the formation of the compound CAIs has been presented by O isotopic distributions (Kim et al., 1998, 2002).

There is some evidence suggesting that chondrules and CAIs are genetically related. The existence of Al-rich chondrules suggests that they contained a small proportion of a CAI-like refractory component in their precursor materials. Sheng et al. (1991) found plagioclase-rich chondrules from the Allende CV3 chondrite. They consist of plagioclase, olivine, pyroxene, and spinel in variable proportions, and their mineral compositions range from plagioclase-rich to olivine-rich. Spinel in some of these chondrules is a relic of their precursor material because it shows a strongly resorbed character (Sheng et al., 1991). Some chondrules retain a chemical signature of fractionation in the solar nebula, i.e., they show positive Ce and Yb anomalies and exhibit strong REE fractionation patterns similar to those of Group II CAIs (Misawa and Nakamura, 1988).

Misawa and Fujita (1994) found a barred-olivine (BO) chondrule R-11 in the Allende meteorite that contains a coarse, subhedral spinel grain ($\sim$200 μm in size) and also includes fassaite, a Ca-Al-rich phase and refractory metal nuggets. This spinel grain may be a relict because its composition is similar to that of CAI spinel. Moreover, Krot and Keil (2002) and Krot et al. (2002) found evidence of CAI-bearing chondrules from

* Author to whom correspondence should be addressed (maruyama@misasa.okayama-u.ac.jp).

primitive carbonaceous chondrites. Some plagioclase-rich chondrules in CR and CH chondrites contain relic CAIs composed of anorthite, spinel, ±Al-diopside, and ±forsterite (Krot and Keil, 2002). Relic CAIs in plagioclase-rich chondrules in reduced CV chondrites are composed of anorthite, spinel, Ca-rich pyroxene, ±forsterite, and ±Al-rich Ca-poor pyroxene (Krot et al., 2002).

These discoveries indicate that CAIs were present in the chondrule-forming regions when chondrules formed. However, the similarities of petrological properties between minerals in CAIs and refractory minerals in chondrules do not always provide sufficient evidence to infer the origin of refractory minerals in chondrules.

Indications that CAI materials were involved in the formation of chondrules are also recorded in trace element compositions and/or isotopic compositions. Oxygen isotopic compositions may provide better tracers of CAI-like materials than REE fractionation patterns, because the minerals of CAIs show large O-isotopic anomalies (e.g., Clayton et al., 1977).

We have analyzed the O isotopic compositions of minerals in two spinel-bearing compound chondrules from the Allende CV chondrite, and found that spinels in the Al-rich chondrule may have originated in CAIs because of their large O isotopic anomaly (Maruyama et al., 1999). These spinel grains were incorporated into chondrule precursors and survived the chondrule-forming event. On the other hand, the spinel grain in the BO chondrule seems to have formed during chondrule crystallization because its O isotopic composition is similar to that of the coexisting olivine bars (Maruyama et al., 1999).

The Al-Mg isotopic composition also potentially provides important information on chondrule formation. The short half-life of ^{26}Al [$\tau_{1/2}$ = 0.72 million years (My)] (Lee et al., 1977), makes it possible to use the Al-Mg system as a relative chronometer of early solar system events (e.g., Russell et al., 1996). Many CAIs show initial abundances of ^{26}Al corresponding to a ^{26}Al/^{27}Al ratio of ~5 × 10^{-5}, while Al-rich chondrules contain only small ^{26}Mg excesses (MacPherson et al., 1995). The paucity of excess ^{26}Mg in Al-rich chondrules may indicate late formation, several My after CAIs (Hutcheon and Jones, 1995). It may be possible to establish the interval between CAI formation and chondrule formation from the Al-Mg isotopic compositions of Al-rich phases in chondrules.

In this paper, we describe the petrological properties, the Al-Mg isotopic compositions and the oxygen isotopic compositions of two Allende compound chondrules of Maruyama et al. (1999), and examine possible relationships between CAIs and chondrules.

2. ANALYTICAL METHODS

2.1. Petrography

Back-scattered electron imaging (BSEI) and quantitative chemical analyses were made for chondrules in two Allende thin sections using a JEOL JSM-5400 scanning electron microscope (SEM) equipped with an Oxford LINK energy dispersive system (EDS) at the University of Tsukuba. The analytical conditions are described in Maruyama et al. (1999). Images of elemental distribution in the chondrules were taken by the SEM-EDS system at the same accelerating voltage and beam current as the quantitative analyses.

2.2. Isotopic Analyses

The two polished thin sections were coated with a ~30 nm gold film to ensure condition and avoid charging under the ion beam of secondary ion mass spectrometry (SIMS). The oxygen isotopic compositions and the Al-Mg isotopic compositions of each mineral phase in the thin sections were determined with the CAMECA IMS-1270 SIMS instrument at Tokyo Institute of Technology.

2.2.1. Oxygen isotopic analysis

Oxygen isotopic measurements were made with a focused positive primary ion beam of cesium with energy of 20 keV. Primary beam currents were adjusted for each run to obtain an ^{16}O$^-$ count rate of ~4 × 10^5 cps. The typical current was ~4 pA and the beam size was 5 μm in diameter. An electron flood gun was used to compensate the electrostatic charging on the sample surfaces. The mass resolution was set to ~6000 (10% valley) to resolve ^{17}O$^-$ from the interference of ^{16}OH$^-$. Measurements were made by scanning through the mass sequences tail of ^{16}O (15.9915 amu), ^{16}O, ^{17}O, ^{16}OH, and ^{18}O in a magnetic peak jumping mode. Additional details are described in Maruyama et al. (1999).

2.2.2. Al-Mg isotopic analysis

Al-Mg isotopic measurements were made with a focused, 23 keV ^{16}O$^-$ beam of 5μm in diameter. Primary beam currents (in the range 0.1 ~ 2.0 nA) were adjusted for each run to obtain a ^{24}Mg or ^{27}Al count rate of ~4 × 10^5 cps. A contrast aperture of 400 μm was used and the energy slit was set to select an energy bandpass of ±75 eV. The field aperture was 2.0 mm, and the mass resolution was set to ~4000 at 10% valley. This was sufficient to resolve all significant interferences from MgH$^+$ as well as other possible molecular and doubly-charged ions. Measurements were made by scanning through the mass sequences ^{24}Mg, ^{25}Mg, ^{26}Mg, and ^{27}Al in a magnetic peak-jumping mode. The counting times for these masses were 2, 6, 6 and 2 s, respectively. Secondary ion signals were detected with an electron multiplier operated in a pulse counting mode. The counts of Al and Mg isotopes were corrected for the deadtime (28±2 ns). A run consisted of 100 cycles through the mass sequence. Isotopic ratios and the standard deviations of a run were computed from the average of all the isotopic ratios.

To correct for the instrumental mass fractionation, a terrestrial anorthite crystal from Miyakejima, Japan, was used as a standard for plagioclase, nepheline and mesostases of chondrules. By comparison of the EDS and the SIMS measurements for anorthite and the mesostases in two chondrules, we found differences of the sensitivity factors for Al/Mg are less than 10% between them. Since we have no appropriate standards for nepheline, we cannot convert ^{27}Al/^{24}Mg secondary ion ratios to ^{27}Al/^{24}Mg atom ratio.

The intrinsic mass fractionation F_{Mg} of the sample is given by F_{Mg} = Δ^{25}Mg$_{unknown}$ $-\Delta^{25}$Mg$_{standard}$, where Δ^{25}Mg expresses the deviation in permil of the ^{25}Mg/^{24}Mg ratio relative to 0.12663 (Catanzaro et al., 1966). The standard was run before and after sample analyses to monitor shifts in the ^{25}Mg/^{24}Mg ratio. Statistical errors (1σ) of Δ^{25}Mg arising from the daily variations of the measurements of the standard were less than ±2.3‰ and typically ±1.3‰. Additional analytical procedures are described in Koike et al. (1993).

3. RESULTS

3.1. Petrography and Chemistry

3.1.1. A1-2b-1 barred-olivine compound chondrule

A1-2b-1 (hereafter abbreviated A1) is a compound chondrule consisting of a BO chondrule surrounded by an enveloping secondary chondrule (Fig. 1). It is ~3 mm in diameter. The BO chondrule mainly consists of olivine and Ca-Al-rich mesostasis. The secondary is a PO chondrule containing many opaque mineral nodules. The remarkable feature is that a coarse spinel grain is embedded in the BO chondrule. The chemical
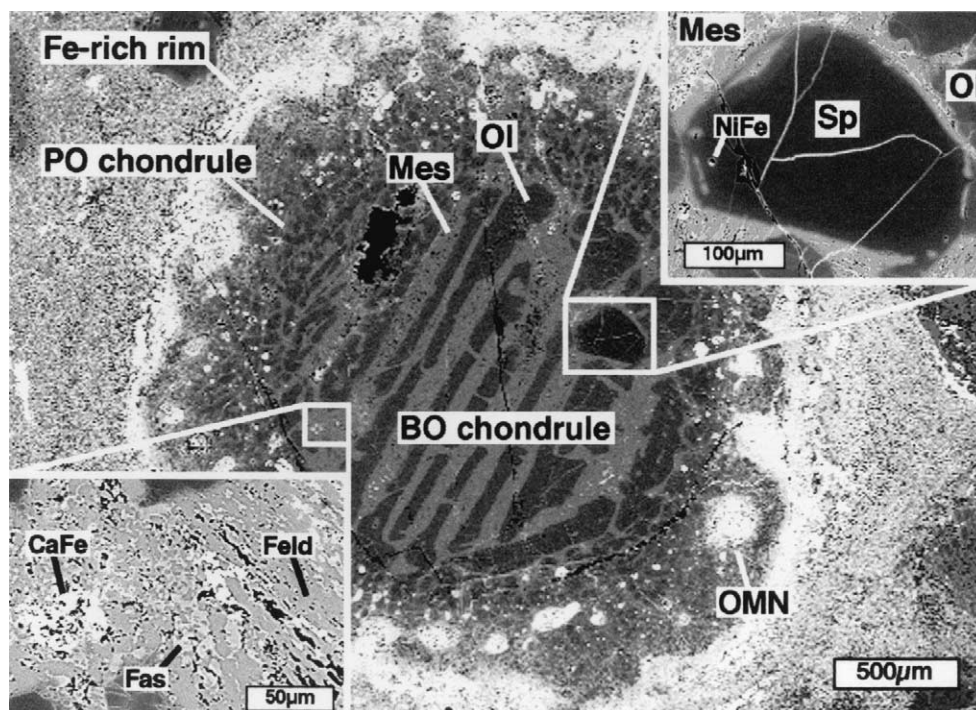
Fig. 1. Back-scattered electron (BSE) image of the A1 compound chondrule from the Allende chondrite consisting of a barred-olivine (BO) primary chondrule surrounded by a PO secondary chondrule (200–500 μm in thickness). A coarse spinel grain is embedded in the BO chondrule. This compound chondrule is surrounded by a Fe-rich fine-grained rim. The PO chondrule mainly consists of porphyritic olivine grains, Ca-poor pyroxene, and opaque mineral nodules. *Sp*: spinel, *Ol*: olivine, *Mes*: mesostasis, *OMN*: opaque mineral nodule, *Feld*: feldspathic phase, *Fas*: fassaitic phase, *CaFe*: Ca-Fe-rich silicate phase, *NiFe*: Ni-Fe metal spherule.

analyses of olivine, spinel, mesostasis and pyroxene of the A1 compound chondrule are given in Table 1.

The central part (~1.7 mm in diameter) shows a typical texture of a BO chondrule. Most olivine bars (~60 μm in width) are parallel to each other. The central part is partially rimmed by an olivine shell (~130 μm in width). The olivine

bars and the olivine shell are forsteritic (Fo$_{98-100}$). The olivines near cracks (>4 μm in width) and grain boundaries (4–6 μm in width) are slightly fayalitic (Fo$_{80-90}$). These Fe-enrichments probably result from Fe diffusion into the olivines during secondary alteration on the parent body. The mesostasis among the olivine bars occupies ~40 vol.% of

Table 1. Representative compositions of minerals in the BO chondrule and the PO chondrule of the A1 compound chondrule.

	BO chondrule						PO chondrule		
	Spinel			Mesostasis			Olivine		
Oxide wt.%	core[a]	rim[b]	Olivine	feldspathic	fassaitic	Ca-Fe-rich	core[a]	rim[b]	Ca-poor Pyroxene
SiO$_2$	0.1	1.8	41.3	44.0	50.0	41.2	40.0	37.8	57.7
TiO$_2$	0.3	0.5	0.2	0.2	3.2	0.1	0.1	0.1	0.2
Al$_2$O$_3$	69.0	64.7	1.1	34.8	8.1	4.9	0.3	0.9	1.0
Cr$_2$O$_3$	0.7	2.8	0.1	0.1	0.8	0.0	0.1	0.8	0.6
MgO	28.9	24.4	54.5	0.8	16.3	1.9	47.3	35.6	36.4
CaO	0.0	1.1	0.8	18.8	18.9	28.4	0.3	0.2	0.9
MnO	0.0	0.1	0.1	0.0	0.1	0.5	0.1	0.2	0.2
FeO	0.6	5.3	1.3	0.6	1.0	21.7	12.5	23.4	2.8
NiO	0.0	0.1	0.1	0.1	0.1	0.1	0.0	0.2	0.1
Na$_2$O	0.0	0.2	0.5	0.6	0.8	0.2	0.5	1.0	0.5
K$_2$O	0.0	0.0	0.0	0.0	0.0	0.0	0.0	0.0	0.0
Oxide Total	99.6	101.0	100.0	100.0	99.3	99.0	101.2	100.2	100.4
			Fo$_{99}$				Fo$_{87}$	Fo$_{73}$	En$_{94}$Wo$_2$Fs$_4$

[a] Core of mineral grain.
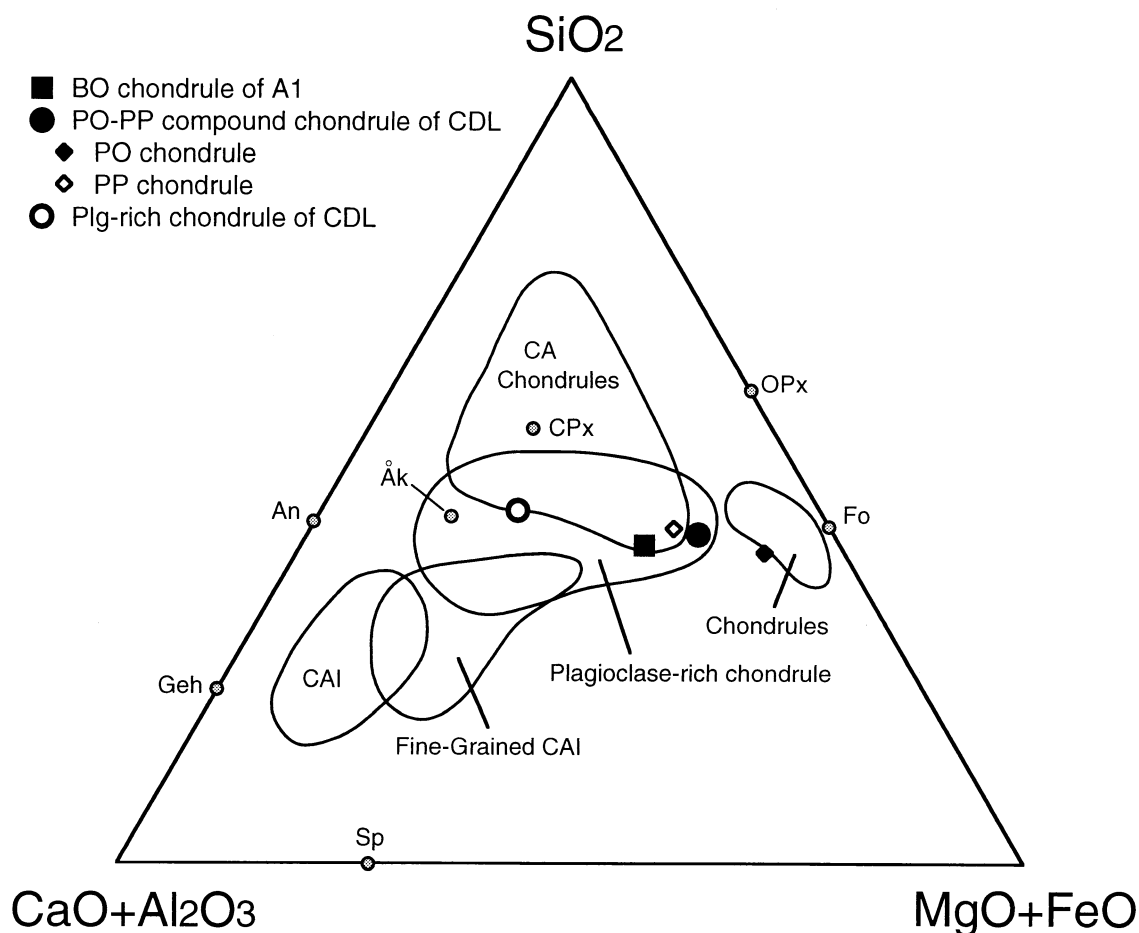[b] Rim of mineral grain.

Fig. 2. The bulk composition of the A1 BO chondrule and three chondrules of CDL. The compositions of minerals which are common in chondrules and CAIs are also plotted for reference. Sources of data are: CAIs from Mason and Martin (1977) and McSween (1977); CA chondrules from Bischoff and Keil (1984); fine-grained CAIs from Brigham (1990) and Mason and Martin (1977); ferromagnesian chondrules from McSween (1977); Plg-rich chondrules from Sheng et al. (1991). The data of the olivine-rich chondrule Redeye was excluded from the data of Plg-rich chondrules. *CA chondrule*: Ca-Al-rich chondrule, *Sp*: spinel, *Fo*: forsterite, *CPx*: Ca-rich pyroxene, *OPx*: Ca-poor pyroxene, *An*: anorthite, *Geh*: gehlenite, *Åk*: åkermanite.

the BO chondrule. The mesostasis can be roughly divided into three components: (1) a feldspathic phase; it resembles feldspar in composition with a slight enrichment in MgO, (2) a minor fassaitic phase scattered throughout the feldspathic phase, and (3) Ca-Fe-rich silicate assemblages; they tend to occur between two former components. Numerous submicron-size grains of Fe, Ni-metal and sulfide are also present in the mesostasis.

The spinel grain is extremely large ($\sim$290 μm in width). Its core is almost pure $MgAl_2O_4$, but the rim is gradually enriched in FeO and Cr_2O_3. The width of the Fe-rich rim ($\sim$7.4 wt.% FeO at the surface) ranges from 4 μm to $\sim$60 μm, whereas the width of the Cr-rich rim ($\sim$3.2 wt.% Cr_2O_3 at the surface) is up to 30 μm. Fe-enrichment near cracks probably results from Fe diffusion into the spinel during secondary alteration on the parent body. The spinel grain contains a Ni-Fe-metal spherule and some Ca-Al-rich silicate patches.

The bulk composition of the BO chondrule is shown in Figure 2. This composition includes the spinel grain. It can be

recognized that the BO chondrule is closely related to Ca-Al-rich chondrules, reflecting the presence of a large amount of Ca-Al-rich mesostasis and the spinel in the BO chondrule. The texture of the BO chondrule is quite different from typical Ca-Al-rich chondrules.

The PO chondrule resembles the igneous rims described by Krot and Wasson (1995). The thickness of the PO chondrule ranges from $\sim$200 μm to $\sim$500 μm. It mainly consists of zoned porphyritic olivine grains ($\sim$25 μm in size) with minor amounts of low-Ca pyroxene ($<$20 μm in size) and opaque mineral nodules. The average forsterite contents of the Mg-rich cores and Fe-rich rims of the porphyritic olivine grains are $\sim$Fo$_{90}$ and $\sim$Fo$_{70}$, respectively. Several small clumps of pyroxene are distributed along the outer part of the PO chondrule. Many opaque mineral nodules are scattered throughout the PO chondrule (10–210 μm in diameter). They mainly consist of Fe-Ni metal and/or sulfides.

The outer rim surrounding the A1 compound chondrule is Fe-rich and fine-grained. It varies in thickness from 60 to 130
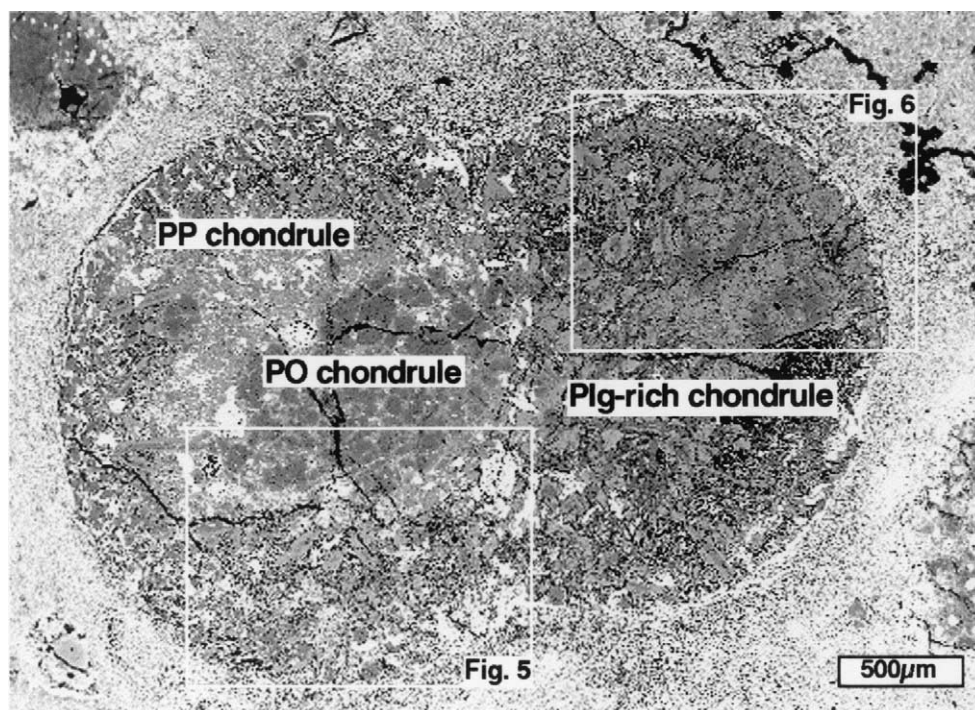
Fig. 3. BSE image of CDL compound chondrule from the Allende chondrite. CDL can be divided into a PO chondrule, a PP chondrule, and a Plg-rich chondrule. The areas of Fig. 5 and Fig. 6 are also shown.

μm. The rim is peppered with silicates (e.g., fayalite). The distribution of sulfides in the outer rim is heterogeneous.

3.1.2. AL95-2-1-CDL.1 compound chondrule

AL95-2-1-CDL.1 (hereafter abbreviated CDL) is also a compound chondrule (Fig. 3). Three chondrules can be recognized within CDL. The first to form was the small, spindle-shaped

(1200 μm × 830 μm) one, the next was the PP chondrule (~770 μm in maximum thickness) that enveloped this. The third was the plagioclase-rich chondrule (hereafter abbreviated Plg-rich chondrule) that adhered to one side of the PO-PP compound chondrule. This third chondrule consists of Ca-Al-rich minerals similar to those in CAIs, and can be categorized as a Plg-rich chondrule as described by Sheng et al. (1991).

Table 2. Representative compositions of minerals in the PO chondrule and the PP chondrule of CDL.

	PO chondrule	PP chondrule						
	Olivine	Olivine (inner region)[a]		Olivine (boundary)[b]		Ca-poor pyroxene	Ca-rich Pyroxene	Anorthite
Oxide wt. %		core[c]	rim[d]	core[c]	rim[d]			
SiO$_2$	41.6	39.8	36.6	37.0	35.3	57.1	52.9	43.3
TiO$_2$	0.1	0.1	0.1	0.1	0.1	0.4	1.3	–
Al$_2$O$_3$	0.1	0.1	0.8	0.4	1.1	1.1	3.5	34.1
V$_2$O$_3$	–	–	–	–	–	0.1	0.1	–
Cr$_2$O$_3$	0.2	0.1	0.4	0.3	0.6	0.6	0.6	–
MgO	55.6	47.9	36.1	36.1	29.0	35.8	22.1	0.5
CaO	0.3	0.3	0.3	0.2	0.3	3.7	18.5	19.2
MnO	0.1	0.1	0.1	0.1	0.2	0.1	0.2	–
FeO	2.3	11.7	25.3	25.9	33.2	0.8	0.8	0.7
NiO	0.1	0.1	0.1	0.1	0.1	–	–	–
Na$_2$O	–	–	–	–	–	–	–	1.1
Oxide Total	100.3	100.2	99.8	100.2	99.8	99.7	100.0	98.8
	Fo$_{98}$	Fo$_{88}$	Fo$_{72}$	Fo$_{71}$	Fo$_{61}$	En$_{92}$Wo$_7$Fs$_1$	En$_{62}$Wo$_{37}$Fs$_1$	An$_{91}$

[a] Olivine grains included within the PP chondrule.
[b] Olivine grains along the boundary between the PP chondrule and the matrix.
[c] Core of olivine grain.
[d] Rim of olivine grain.

Table 3. Representative compositions of unaltered minerals in the Plg-rich chondrule of CDL.

| Oxide wt.% | Spinel (spinel cluster) | | Spinel | Olivine (core)[b] | | Olivine (core-rim)[c] | | Ca-poor pyroxene | Ca-rich pyroxene | Anorthite |
	core-side[d]	rim-side[e]	(rim)[a]	core[f]	rim[g]	core[f]	rim[g]			
SiO₂	0.4	0.4	0.5	41.1	40.3	40.3	37.8	56.6	52.8	43.0
TiO₂	1.7	1.3	1.0	0.2	0.2	0.1	0.2	0.6	1.5	–
Al₂O₃	64.4	60.9	60.7	0.3	0.3	0.1	0.5	1.5	3.3	35.6
V₂O₃	0.4	0.4	0.5	–	–	–	–	0.1	0.1	–
Cr₂O₃	2.2	2.0	2.0	0.2	0.3	0.1	0.7	0.7	0.7	–
MgO	25.8	17.4	16.6	53.3	51.2	47.1	38.9	34.3	22.1	0.3
CaO	0.2	0.0	0.2	0.3	0.3	0.3	0.3	5.1	18.5	20.1
MnO	–	–	–	0.1	0.1	0.1	0.1	0.1	0.2	–
FeO	3.9	16.4	17.7	4.6	6.9	12.3	22.1	0.7	0.7	0.5
NiO	–	–	–	0.1	0.1	0.0	0.1	–	–	–
Na₂O	–	–	–	–	–	–	–	–	–	0.5
Oxide Total	99.0	98.9	99.2	100.2	99.6	100.3	100.6	99.7	99.9	99.9
				Fo₉₅	Fo₉₃	Fo₈₇	Fo₇₆	En₉₂Wo₇Fs₁	En₆₂Wo₃₇Fs₁	An₉₆

[a] Spinel grains in the rim arc.
[b] Olivine grains in the core part of the Plg-rich chondrule.
[c] Olivines along the boundary between the core and the rim arc.
[d] Spinel existing away from the rim arc.
[e] Spinel existing near the rim arc.
[f] Core of olivine grain.
[g] Rim of olivine grain.

Following Wasson et al. (1995), CDL can be categorized as an "independent" compound chondrule consisting of primary and secondary members. The PO-PP chondrule can be categorized as an "enveloping" (the secondary encloses the primary) compound chondrule, and the relationship between the PO-PP and the Plg-rich chondrule can be considered as a "consorting" (secondary subequal to primary in size and shape) compound chondrule.

The bulk composition of each CDL chondrule is also shown in Figure 2. The PO chondrule has a composition on the edge of the field of normal ferromagnesian chondrules, whereas the composition of the PP chondrule overlaps with Ca-Al-rich chondrules due to abundant Ca-rich pyroxene. The bulk composition of the Plg-rich chondrule overlaps with those reported by Sheng et al. (1991) and Ca-Al-rich chondrules. The Plg-rich chondrule contains a large amount of Na₂O (8.3 wt.% Na₂O) because of abundant nepheline (~30 vol.%). Representative chemical compositions of minerals in the PO chondrule and the PP chondrule are given in Table 2. Representative chemical compositions of minerals in the Plg-rich chondrule are given in Table 3 except for nepheline.

The distribution of volatile elements in CDL is shown in Figure 4. The most characteristic feature is the Cl-zonation (Fig. 4a). This indicates that CDL experienced extensive secondary alteration. CDL can be roughly divided into two parts: an outer Cl-bearing zone (370–450 μm in width) and a Cl-poor zone (Fig. 4a). Representative chemical compositions of the mesostasis and nephelines in CDL are given in Table 4.

The texture of the PO chondrule is shown in Figure 5. It mainly consists of porphyritic olivine grains (~Fo₉₈) that range from ~40 μm to ~210 μm in diameter. The mesostasis (~6 vol.%) is feldspathic and scarcely contains Na, K, and Cl (Table 4). Many opaque nodules are arranged along the boundary between the PO and PP chondrules. There are a few Fe-Ni sulfide blebs in the PO chondrule.
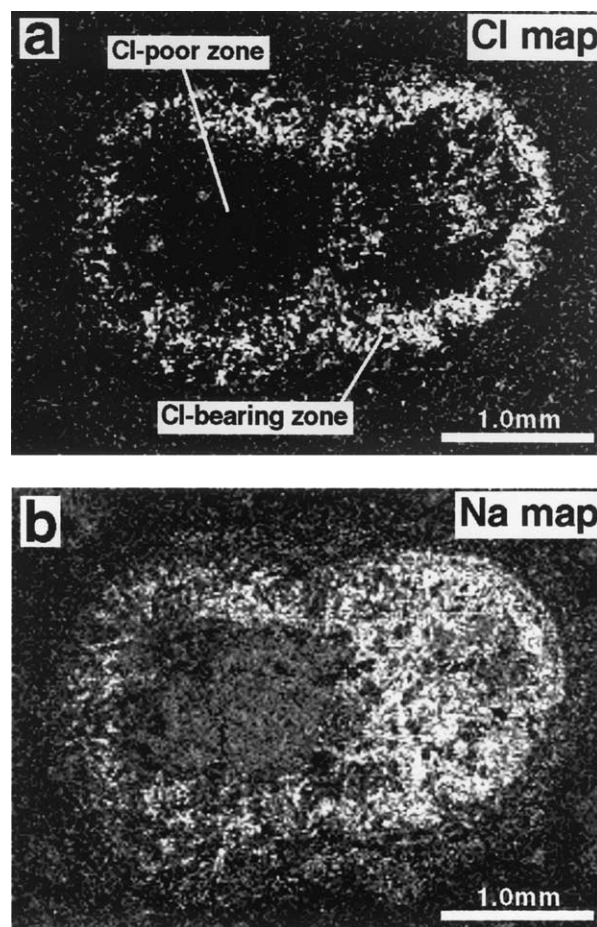

Fig. 4. The distribution of chlorine (a) and sodium (b) in CDL. CDL can be divided into Cl-bearing zone and Cl-poor zone. The PP and the Plg-rich chondrules contain sodium in the mesostasis and in nepheline, whereas the PO chondrule is Na-Cl-poor. The Na and Cl distribution are similar in the PO chondrule but quite different in the Plg-rich chondrules.

Table 4. Mean compositions of mesostasis and nephelines in CDL.

wt.%	PO chondrule mesostasis	PP chondrule mesostasis		Plg-rich chondrule[a] nepheline		
		Cl-poor[b]	Cl-bearing[c]	Cl-poor[b]	Cl-bearing[c]	rim arc
SiO_2	46.3	45.0	38.1	42.3	36.8	41.2
Al_2O_3	30.3	31.1	31.8	34.3	33.0	34.8
MgO	3.1	1.7	0.8	–	–	–
CaO	16.3	12.7	2.3	2.5	1.1	4.5
FeO	1.5	1.6	1.9	0.4	2.1	0.5
Na_2O	2.0	6.9	20.2	18.0	20.6	17.1
K_2O	0.0	0.4	0.9	1.7	0.3	1.8
Oxide Total	99.4	99.4	96.0	99.1	93.9	100.0
Cl	0.0	0.5	3.9	0.9	6.1	0.0

[a] Values of oxides and Cl were normalized to (oxides + Cl) = 100 wt.%.
[b] Cl-poor zone.
[c] Cl-bearing zone.

The texture of the PP chondrule is also shown in Figure 5. The PP chondrule mainly consists of coarse Ca-rich pyroxenes in the interior and coarse Ca-poor pyroxene near the surface; there is also a small amount of olivine. A large amount of Ca-rich pyroxene (78 vol.% of pyroxenes) is present. Most Ca-poor pyroxenes have a porphyritic appearance (40–70 μm in maximum diameter), while Ca-rich pyroxenes exhibit the appearance of laths (90–370 μm in length). Some pyroxene laths can be divided into Ca-poor pyroxene cores and Ca-rich pyroxene mantles. Ca-rich pyroxenes contain small amounts of Al_2O_3 (~3.5 wt.%) and TiO_2 (~1.3 wt.%). Ca-poor pyroxenes contain ~1.1 wt.% Al_2O_3 and ~0.4 wt.% TiO_2. Both of Ca-rich and Ca-poor pyroxenes are Fe-poor (Fs_1), and show no Fe-Mg zoning. The olivine grains range from ~40 to ~100 μm in diameter. Those that lie along the boundary between the PP chondrule and the matrix are fayalitic (Fo_{61-71}). The olivine grains in the inner region show Fe-Mg zoning, with cores ~Fo_{88}, and rims ~Fo_{72}. Most of the mesostasis in the PP chondrule is in the Cl-bearing zone, but a small amount of the mesostasis near the PO chondrule is in the Cl-poor zone. A
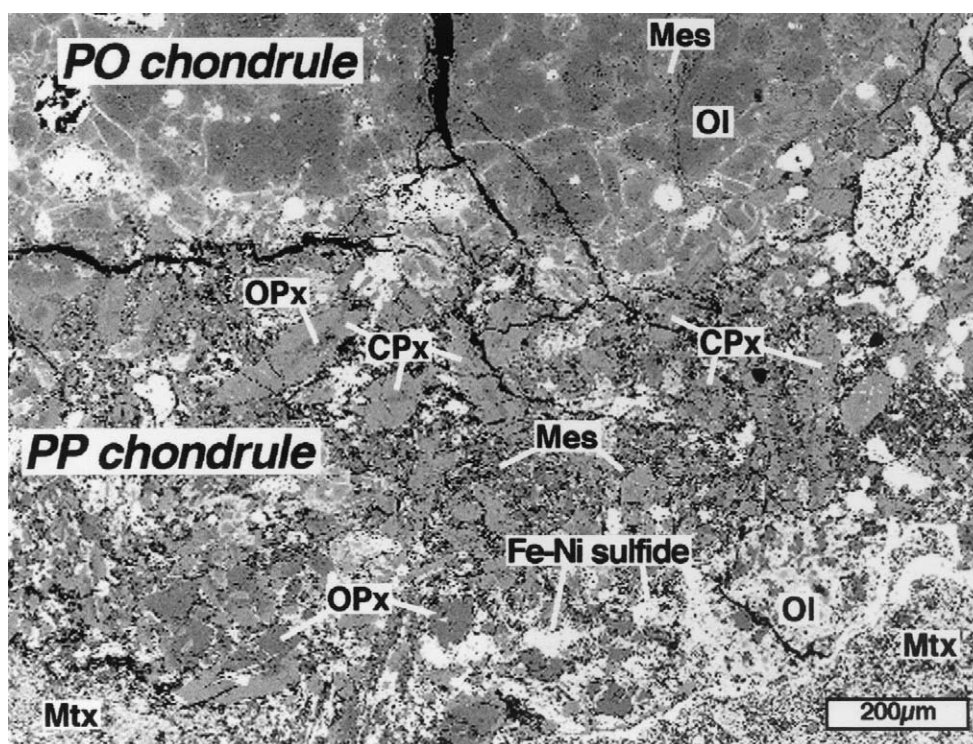

Fig. 5. BSE image of the PO-PP compound chondrule of CDL. Porphyritic olivine grains dominate the PO chondrule. The PP chondrule consists of pyroxene with a small amount of olivine. *Ol*: olivine, *CPx*: Ca-rich pyroxene, *OPx*: Ca-poor pyroxene, *Mes*: mesostasis, *Mtx*: matrix.
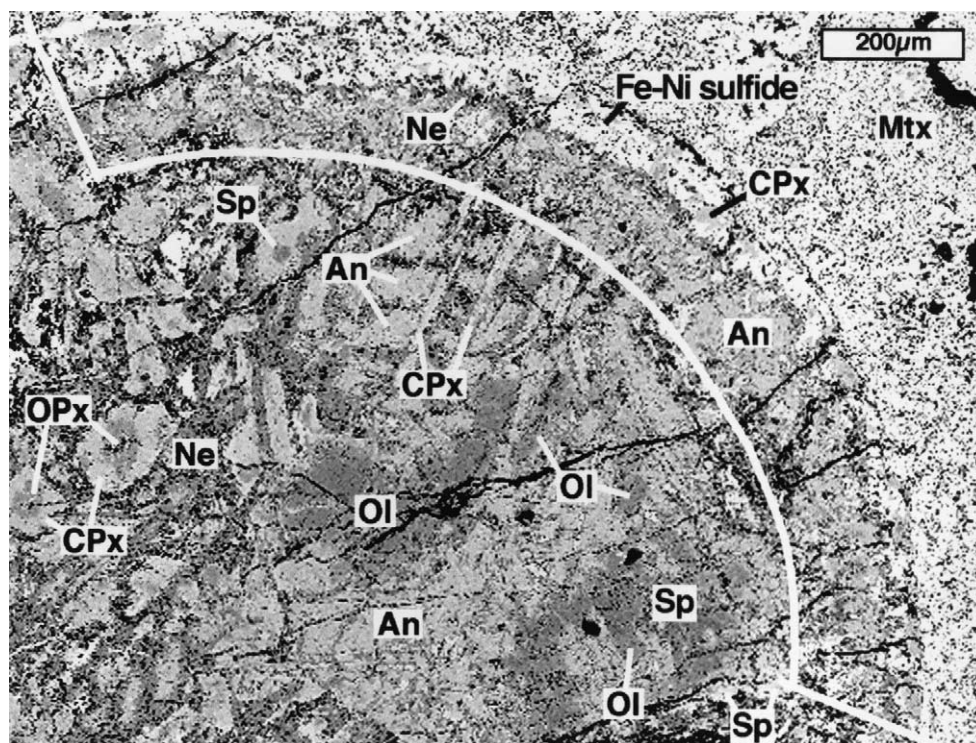
Fig. 6. BSE image of the Plg-rich chondrule of the CDL. The Plg-rich chondrule is subophitic, and consists of pyroxene, plagioclase, olivine, spinel, and nepheline. The range of the rim arc is shown by a solid line. *Sp*: spinel, *Ol*: olivine, *CPx*: Ca-rich pyroxene, *OPx*: Ca-poor pyroxene, *An*: anorthite, *Ne*: nepheline, *Mtx*: matrix.

minor amount of plagioclase occurs at the boundary between the primary chondrule and the Plg-rich chondrule.

The Plg-rich chondrule is spheroidal (1900 μm $\times$ 1400 μm). It consists of pyroxene, plagioclase, olivine, spinel and nepheline. The mineral composition resembles that of the Group-2 Plg-rich chondrule of Sheng et al. (1991); it contains minor spinel ($<5\%$) and abundant plagioclase (30–60%). The texture of the core is subophitic (Fig. 6). Olivines, pyroxenes and spinel grains are poikilitically enclosed by the plagioclase assemblage. Nepheline is a major constituent ($\sim$30 vol.%) and exists as a matrix surrounding other phases. Nepheline was apparently formed by alteration of plagioclase. A similar occurrence of nepheline in Allende chondrules has been observed by Ikeda and Kimura (1995). Thus it appears that plagioclase originally occupied more than half of the Plg-rich chondrule before the secondary alteration occurred.

A multilayered rim arc (hereafter shortened "rim arc") partially surrounds the Plg-rich chondrule. This structure is found in the portion shown in Figure 6 only. This portion of the rim can be roughly divided from the outside to the inside into a pyroxene layer and Fe-Ni sulfide ($\sim$70 μm in width), a nepheline layer ($\sim$20 μm), and a plagioclase layer peppered with hercynitic spinel grains ($\sim$80 μm).

Randomly oriented pyroxene laths dominate the Plg-rich chondrule ($\sim$34 vol.%). The texture and the chemical composition of the pyroxenes are quite similar to those of pyroxenes in the PP chondrule. Both Ca-rich and Ca-poor pyroxenes are Fe-poor (Fs_1), and show no Fe-Mg zoning. The plagioclase occupies $\sim$25 vol.% of the Plg-rich chondrule. Plagioclase laths are abundant near the rim arc. Plagioclase (An_{88-100})

contains a small amount of MgO (<0.7 wt.%) and FeO (0.2–1.6 wt.%). Nephelines in the Cl-bearing zone contain 5–8 wt.% Cl, and scarcely contains potassium. Nephelines in the Cl-poor zone and the rim arc contain a small amount of Cl and much more K (Table 4). Nephelines among plagioclase laths inside the Cl-bearing zone are Cl-rich (2.7–7.0 wt.% Cl) and K-poor (<0.8 wt.% K_2O). Olivine is a minor phase ($\sim$4 vol.%) in the Plg-rich chondrule. Olivine grains are enclosed by plagioclase laths, and some are in contact with Ca-rich pyroxenes or spinels. Most olivines are porphyritic, and some of them are elongated (20–180 μm in long dimension). Their cores are forsteritic ($\sim Fo_{95}$), and the rims are slightly Fe-rich ($\sim Fo_{93}$). The olivine grains at the boundary between the core and the rim arc are Fe-richer. The average compositions of the core and the rim of these olivines are Fo_{87} and Fo_{76}, respectively.

Spinels in the Plg-rich chondrule exist in the rim arc and in the plagioclase assemblage (Fig. 7). Many spinel grains show a strongly corroded texture, which is a characteristic of spinels in Group-2 plagioclase-rich chondrules (Sheng et al., 1991). The spinel cluster (Fig. 7a) in the core of the Plg-rich chondrule contains 0.6–2.8 wt.% Cr_2O_3 and 0.4–3.0 wt.% TiO_2; distributions of Cr and Ti exhibit no systematic zonation. Iron in the spinel cluster is zoned; grains far away from the rim arc are Fe-poor (2–8 wt.% FeO), while those near the rim arc are Fe-rich (13–20 wt.% FeO). One isolated spinel grain (Fig. 7b) has Fe-Mg zonal structure. Unfortunately, the zone is too thin to allow a quantitative analysis. Many spinel grains inside the rim arc are subhedral with sizes ranging from $\sim$6 to $\sim$20 μm, and some of them show a strongly corroded appearance (Fig. 7c). These spinel grains are Fe-rich (8–19 wt.% FeO).
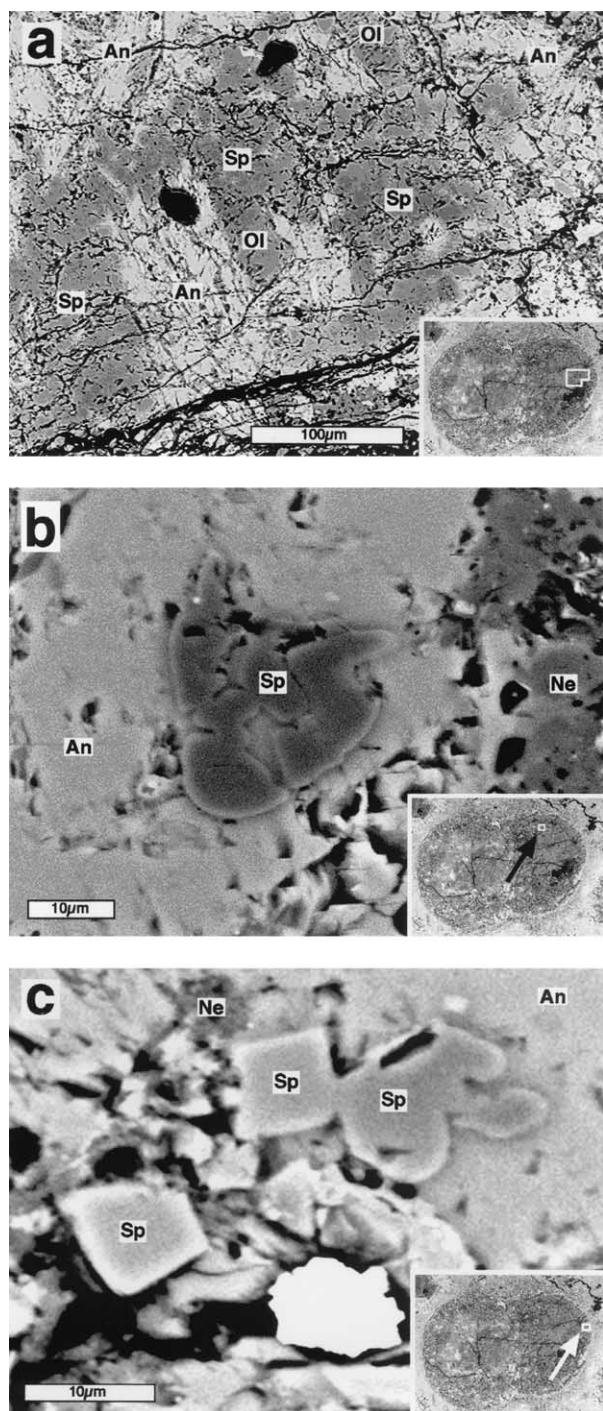
Fig. 7. BSE images of the spinel grains in the Plg-rich chondrule of CDL. The spinel grains show a corroded appearance. (a) The spinel cluster in the plagioclase assemblage. (b) The isolated spinel grain in the plagioclase assemblage. (c) The spinel grains in the rim arc of the Plg-rich chondrule. The spinel grain in the upper right of the image shows a strongly corroded appearance. *Sp*: spinel, *Ol*: olivine, *An*: anorthite, *Ne*: nepheline.

3.2. Oxygen Isotopic Compositions

The results of oxygen isotopic analysis for the major phases in the A1 BO chondrule and CDL are summarized in Table 5,

including previous published data (Maruyama et al., 1999). As shown in Figure 8, the oxygen isotopic composition of all phases lie near the mass-independent CCAM (Carbonaceous Chondrite Anhydrous Minerals) mixing line defined by Clayton et al. (1983). The mean $\Delta^{17}O$ value of olivines is $-5.6\pm0.8‰$. Similar ^{16}O-excesses have been observed in individual olivine grains (Hervig and Steele, 1992; Weinbruch et al., 1993) and in olivines of a PO chondrule from the Allende meteorite (Hiyagon, 1997). The mean $\Delta^{17}O$ values of the core and the rim of the spinel grain are $-6.4\pm0.9‰$ and $-8.4\pm1.9‰$, respectively. There is no discernible difference in O isotopic composition between the core and the rim. The O isotopic composition of the spinel grain in the A1 BO chondrule is similar to that of spinel in an Al-rich chondrule from Sharp H3.4 chondrite (Russell et al., 2000). The $\Delta^{17}O$ value of the feldspathic mesostasis is $-0.6\pm1.4‰$, which is close to that of plagioclase in CAIs from CV3 meteorites (Clayton et al., 1977).

The oxygen isotopic composition of all phases in CDL also lie near the CCAM line (Fig. 9). The $\Delta^{17}O$ value of an olivine in the PO chondrule is $-8.6\pm3.3‰$. The $\Delta^{17}O$ value of olivines in the Plg-rich chondrule is $-10.4\pm1.0‰$. The olivine in CDL is slightly enriched in ^{16}O compared to olivine in the A1 BO chondrule. The mean $\Delta^{17}O$ values of Ca-poor pyroxenes in the PP chondrule and in the Plg-rich chondrule are $-5.8\pm1.6‰$ and $-5.3\pm1.6‰$, respectively. The $\Delta^{17}O$ value of a Ca-rich pyroxene in the PP chondrule is $-7.1\pm3.2‰$, and the mean $\Delta^{17}O$ value of Ca-rich pyroxene in the Plg-rich chondrule is $-5.4\pm0.7‰$. There is no obvious difference in $\Delta^{17}O$ values between Ca-rich pyroxene and Ca-poor pyroxene in the PP chondrule and in the Plg-rich chondrule. The mean $\Delta^{17}O$ value of plagioclase grains in the Plg-rich chondrule is $-2.4\pm0.9‰$, close to that of plagioclase in CAIs from CV3 meteorites (Clayton et al., 1977). The mean $\Delta^{17}O$ value of nepheline is $-5.7\pm1.3‰$, thus, nepheline is slightly enriched in ^{16}O compared to plagioclase. The mean $\Delta^{17}O$ value of spinel in the Plg-rich chondrule is $-17.3\pm2.0‰$, greatly different from those of spinels in the Al-rich chondrules ($-6 \sim -1‰$) in unequilibrated ordinary chondrites observed by Russell et al. (2000). The $\Delta^{17}O$ value of spinel is comparatively close to that of spinel in typical Type B CAIs ($\Delta^{17}O \approx -21‰$) in the Allende meteorite (Clayton et al., 1977). The spinel is anomalous with respect to oxygen isotopes compared to the other phases in CDL.

3.3. Magnesium Isotopic Compositions

The magnesium isotopic data were obtained on the feldspathic mesostasis in the A1 BO chondrule, the PO chondrule of CDL, and plagioclases and nephelines in the Plg-rich chondrule of CDL. The primary purpose was to establish the presence of an isotopic effect due to radiogenic excess of ^{26}Mg ($^{26}Mg*$) from ^{26}Al decay. The Mg isotopic measurements are summarized in Table 6. Since secondary ion intensity ratios of $^{27}Al/^{24}Mg$ for the nepheline in the Plg-rich chondrule were large and the MgO contents were below detection limits (<0.1 wt.%), it is concluded that nepheline shows no resolvable $^{26}Mg*$.

The correlation of $\delta^{26}Mg$ with the $^{27}Al/^{24}Mg$ ratio for the feldspathic mesostasis in the A1 BO chondrule is shown in Figure 10. The best-fit slope of the correlation line for all the

Table 5. Oxygen isotopic compositions (permil) of the major phases of the A1 BO chondrule and CDL.

Analysis	$\delta^{17}O_{SMOW}$ ($\pm 1\sigma_{mean}$)	$\delta^{18}O_{SMOW}$ ($\pm 1\sigma_{mean}$)	$\Delta^{17}O$ ($\pm 1\sigma_{mean}$)
A1 Spinel			
SpC01[ab]	-13.8 ± 2.8	-8.9 ± 2.1	-9.2 ± 3.0
SpC02[ab]	-14.8 ± 3.2	-13.8 ± 2.0	-7.6 ± 3.4
SpC03[ab]	-15.6 ± 3.1	-12.9 ± 1.9	-8.9 ± 3.3
SpC04	-14.6 ± 2.6	-16.0 ± 1.8	-6.3 ± 2.8
SpC05	-14.2 ± 2.5	-17.2 ± 2.0	-5.2 ± 2.7
SPC06	-14.4 ± 3.2	-16.7 ± 2.2	-5.7 ± 3.4
SpC07	-7.2 ± 3.0	-10.2 ± 1.9	-1.9 ± 3.2
SpR01[ab]	-10.0 ± 3.0	-12.3 ± 2.0	-3.6 ± 3.2
SpR03	-21.2 ± 3.2	-16.9 ± 2.1	-12.4 ± 3.3
SpR04	-19.0 ± 3.0	-22.2 ± 2.1	-7.5 ± 3.2
SpR05[a]	-14.9 ± 3.0	-8.8 ± 2.0	-10.3 ± 3.2
Average	-14.5 ± 1.1	-14.2 ± 1.2	-7.1 ± 0.9
A1 Olivine			
O101(Fo99)	-17.5 ± 3.3	-10.2 ± 2.0	-12.2 ± 3.5
O102(Fo100)	-8.1 ± 3.2	-5.1 ± 2.1	-5.4 ± 3.3
O103(Fo99)	-14.2 ± 3.1	-11.6 ± 2.1	-8.2 ± 3.3
O104(Fo100)	-9.9 ± 3.3	-13.2 ± 1.9	-3.1 ± 3.5
O105(Fo100)	-7.7 ± 3.1	-10.2 ± 2.2	-2.4 ± 3.3
O106(Fo100)[a]	-3.2 ± 3.2	-1.3 ± 1.8	-2.5 ± 3.3
O107(Fo100)	-8.6 ± 2.6	-6.7 ± 1.9	-5.1 ± 2.8
O108(Fo99)	-9.2 ± 3.3	-7.4 ± 2.3	-5.4 ± 3.5
O109(Fo99)	-5.0 ± 2.9	-5.5 ± 2.1	-2.2 ± 3.1
O110(Fo99)[a]	-11.5 ± 2.9	-8.1 ± 2.1	-7.3 ± 3.1
O111(Fo100)[a]	-13.3 ± 2.7	-11.6 ± 2.5	-7.3 ± 3.0
O112(Fo100)	-10.4 ± 3.0	-13.9 ± 2.1	-3.2 ± 3.2
O113(Fo99)	-10.0 ± 3.2	-2.4 ± 2.0	-8.8 ± 3.4
Average	-9.9 ± 1.0	-8.2 ± 1.1	-5.6 ± 0.8
A1 Mesostasis			
Meso01[a]	-1.7 ± 2.8	2.8 ± 2.0	-3.2 ± 3.0
Meso02[a]	0.4 ± 3.3	5.6 ± 1.9	-2.5 ± 3.4
Meso03	-4.2 ± 2.7	3.5 ± 2.0	-6.0 ± 2.9
Meso04	-0.6 ± 2.5	-1.6 ± 2.1	0.3 ± 2.8
Meso05	5.0 ± 3.0	2.3 ± 2.1	3.8 ± 3.1
Meso06[a]	4.0 ± 2.6	7.5 ± 2.0	0.1 ± 2.8
Meso07	9.2 ± 2.9	10.7 ± 2.1	3.7 ± 3.1
Average	1.7 ± 1.7	4.4 ± 1.5	-0.6 ± 1.4
Spinel CDL (Plg-rich chondrule)			
Sp01[a]	-33.0 ± 2.9	-28.8 ± 2.0	-18.1 ± 3.1
Sp02[a]	-35.8 ± 2.9	-32.5 ± 2.0	-18.8 ± 3.0
Sp03[a]	-32.6 ± 2.7	-29.1 ± 2.1	-17.5 ± 2.9
Sp04[a]	-34.3 ± 3.1	-23.6 ± 1.9	-22.0 ± 3.2
Sp05[a]	-27.9 ± 3.0	-34.1 ± 1.8	-10.1 ± 3.1
Average	-32.7 ± 1.3	-29.6 ± 1.8	-17.3 ± 2.0
Olivine CDL (Plg-rich chondrule)			
O101 (Fo97)[a]	-20.2 ± 3.1	-19.3 ± 2.3	-10.2 ± 3.3
O102 (Fo96)[a]	-16.3 ± 3.2	-12.4 ± 2.2	-9.8 ± 3.4
O103 (Fo96)	-14.5 ± 3.1	-12.9 ± 2.0	-7.8 ± 3.3
O104 (Fo97)	-18.0 ± 3.2	-13.2 ± 1.9	-11.1 ± 3.3
O105 (Fo98)	-25.1 ± 3.0	-19.4 ± 1.9	-15.0 ± 3.1
O106 (Fo98)	-13.4 ± 2.8	-9.5 ± 2.4	-8.5 ± 3.1
Average	-17.9 ± 1.7	-14.5 ± 1.6	-10.4 ± 1.0
Ca-rich Pyroxene CDL (Plg-rich chondrule)			
ssCPx01	-13.7 ± 2.7	-13.1 ± 1.9	-6.9 ± 2.9
ssCPx02	-8.2 ± 3.1	-6.4 ± 2.2	-4.9 ± 3.3
ssCPx03	-11.3 ± 3.1	-7.8 ± 1.8	-7.2 ± 3.2
ssCPx04[a]	-11.3 ± 3.2	-8.8 ± 2.0	-6.7 ± 3.3
ssCPx05	-8.4 ± 2.8	-10.7 ± 2.1	-2.9 ± 3.0
ssCPx06	-10.4 ± 2.7	-12.5 ± 1.9	-3.9 ± 2.9
Average	-10.5 ± 0.8	-9.9 ± 1.1	-5.4 ± 0.7
Ca-poor Pyroxene CDL (Plg-rich chondrule)			
ssOPx01[a]	-11.2 ± 2.7	-10.4 ± 1.9	-5.8 ± 2.9
ssOPx02	-4.9 ± 2.8	-3.4 ± 2.2	-3.2 ± 3.0
ssOPx03	-7.5 ± 3.0	-9.2 ± 1.8	-2.7 ± 3.2
ssOPx04	-12.8 ± 2.6	-6.3 ± 2.1	-9.5 ± 2.8
Average	-9.1 ± 1.8	-7.3 ± 1.6	-5.3 ± 1.6
			(Continued)

Table 5. (Continued)

Analysis	$\delta^{17}O_{SMOW}$ ($\pm 1\sigma_{mean}$)	$\delta^{18}O_{SMOW}$ ($\pm 1\sigma_{mean}$)	$\Delta^{17}O$ ($\pm 1\sigma_{mean}$)
Anorthite CDL (Plg-rich chondrule)			
An01	-2.7 ± 3.1	3.2 ± 1.8	-4.3 ± 3.2
An02	-3.7 ± 2.9	1.2 ± 2.3	-4.3 ± 3.1
An03	0.4 ± 3.4	0.9 ± 2.1	-0.1 ± 3.6
An04[a]	-5.6 ± 3.0	-1.5 ± 2.1	-4.8 ± 3.2
An05	-1.9 ± 3.1	-1.6 ± 1.9	-1.1 ± 3.2
An06	1.3 ± 3.2	2.1 ± 1.9	0.2 ± 3.4
Average	-2.0 ± 1.0	0.7 ± 0.8	-2.4 ± 0.9
Nepheline CDL (Plg-rich chondrule)			
Ne01	-4.3 ± 2.8	-0.1 ± 2.4	-4.3 ± 3.1
Ne02	-8.5 ± 2.7	-2.7 ± 2.1	-7.1 ± 2.9
Ne03	-7.3 ± 3.2	2.3 ± 2.0	-8.4 ± 3.3
Ne04[a]	-4.0 ± 3.0	-2.0 ± 2.0	-3.0 ± 3.2
Average	-6.0 ± 1.1	-0.6 ± 1.1	-5.7 ± 1.3
Olivine CDL (PO chondrule)			
psO101 (Fo98)[b]	-14.2 ± 3.1	-10.8 ± 2.1	-8.6 ± 3.3
Ca-rich Pyroxene CDL (PP chondrule)			
psCPx01[a]	-14.0 ± 3.0	-13.2 ± 2.1	-7.1 ± 3.2
Ca-poor Pyroxene CDL (PP chondrule)			
psOPx01[a]	-13.7 ± 3.0	-11.6 ± 1.9	-7.6 ± 3.2
psOPx02	-10.3 ± 3.5	-6.5 ± 1.8	-6.9 ± 3.6
psOPx03	-7.3 ± 3.0	-8.8 ± 2.1	-2.7 ± 3.2
Average	-10.4 ± 1.9	-9.0 ± 1.5	-5.8 ± 1.6

[a] Data published by Maruyama et al. (1999).
[b] Data was recalculated because data published on Maruyama et al. (1999) were miscalculated.

data corresponds to $(^{26}Al/^{27}Al)_0 = [1.6 \pm 9.8(2\sigma)] \times 10^{-6}$. The mesostasis essentially shows no resolvable $^{26}Mg^*$.

The correlation of $\delta^{26}Mg$ with the $^{27}Al/^{24}Mg$ ratio for plagioclase in the Plg-rich chondrule is also shown in Figure 10. Plagioclase data indicate presence of some $^{26}Mg^*$. The best-fit slope of the correlation line for plagioclases corresponds to $(^{26}Al/^{27}Al)_0 = [4.6 \pm 4.0(2\sigma)] \times 10^{-6}$. This is consistent with those of CV chondrules studied by Sheng et al. (1991). The best-fit slope of the correlation line for the mesostasis corresponds to $(^{26}Al/^{27}Al)_0 = [5.3 \pm 19.0(2\sigma)] \times 10^{-6}$ indicating no detectable $^{26}Mg^*$.

4. DISCUSSION

4.1. Secondary Alteration Processes of Chondrules

4.1.1. A1 barred-olivine compound chondrule

The A1 BO chondrule suffered minimal alkali metasomatic alteration, because the mesostasis contains relatively little Na and K. However, the Al-Mg isochron of the feldspathic mesostasis is disturbed (Fig. 10). The Allende meteorite shows evidence of aqueous alteration (e.g., Krot et al., 1995; Kojima and Tomeoka, 1996; Choi et al., 1997), therefore the disturbed isochron may result from aqueous alteration on the parent body. The feldspathic mesostasis ($\Delta^{17}O = -0.6 \pm 1.4$‰) may not have preserved the original oxygen isotope ratio of the chondrule melt at solidification. The glassy mesostasis was decomposed into present mesostasis phases by aqueous or thermal metamorphism. The high $\Delta^{17}O$ value of mesostasis might have been obtained during such events.

The fayalitic rims of olivines in the PO and BO chondrules and the iron-rich cracks in the spinel grain and in the olivine

Table 6. Al-Mg isotopic compositions (permil) of the feldspathic mesostasis, plagioclase, and nepheline in the A1 BO chondrule and CDL.

Analysis	F_{Mg} ($\pm 2\sigma_{mean}$)	$\delta^{26}Mg$ ($\pm 2\sigma_{mean}$)	$^{27}Al/^{24}Mg$ ($\pm 2\sigma_{mean}$)
A1 Feldspathic Mesostasis			
Meso01	−6.6 ± 4.3	7.3 ± 6.8	76.9 ± 7.1
Meso02	−7.1 ± 4.5	7.0 ± 7.3	72.6 ± 3.0
Meso03	−1.3 ± 4.4	−1.1 ± 7.4	100.9 ± 3.5
Meso04	−2.0 ± 3.0	2.4 ± 3.3	19.1 ± 1.7
Meso05	−0.3 ± 5.7	3.7 ± 10.7	215.9 ± 6.8
Meso06	0.3 ± 3.4	−0.9 ± 4.1	33.2 ± 0.6
Meso07	−5.8 ± 3.4	6.7 ± 4.4	38.5 ± 2.1
CDL (Plg-rich chondrule) Plagioclase			
P101	−1.9 ± 5.7	6.3 ± 7.1	99.4 ± 5.8
P102	−2.1 ± 5.4	0.0 ± 6.2	65.4 ± 3.5
P104	−2.0 ± 6.2	10.5 ± 9.0	163.4 ± 4.4
P105	−4.4 ± 6.8	4.4 ± 9.9	126.0 ± 5.2
P106	−6.6 ± 6.5	6.9 ± 11.5	176.7 ± 14.7
P110	−4.3 ± 6.0	6.3 ± 10.7	180.2 ± 5.3
P111	−4.4 ± 5.0	6.9 ± 8.5	123.0 ± 12.7
P112	−1.6 ± 5.8	4.2 ± 11.3	175.2 ± 15.8
P113	−3.7 ± 5.5	5.3 ± 10.2	197.3 ± 11.0
P114	2.5 ± 3.6	2.3 ± 4.6	34.5 ± 3.1
P115	0.5 ± 5.3	0.2 ± 9.8	140.1 ± 9.6
P116	−1.2 ± 4.9	9.0 ± 8.2	89.5 ± 4.6
P117	−9.0 ± 6.1	9.4 ± 11.9	188.4 ± 17.1
CDL (Plg-rich chondrule) Nepheline[a]			
Ne01	0.7 ± 4.2	−2.0 ± 6.4	(73.2 ± 3.3)
Ne02	1.5 ± 4.8	−1.7 ± 8.1	(92.6 ± 6.0)
Ne03	−2.1 ± 8.4	3.3 ± 18.7	(476.9 ± 29.5)
Ne05	−1.1 ± 3.4	−1.1 ± 4.3	(41.7 ± 1.0)
Ne06	−2.2 ± 6.3	−3.5 ± 12.0	(219.1 ± 15.3)
Ne07	1.0 ± 3.9	−0.9 ± 5.5	(61.1 ± 2.5)
CDL (PO chondrule) Mesostasis			
Meso01	−0.9 ± 4.5	1.8 ± 7.2	99.6 ± 5.6
Meso02	−0.6 ± 4.3	7.4 ± 7.4	121.9 ± 4.8
Meso03	−0.1 ± 3.9	3.5 ± 6.6	52.2 ± 3.1

[a] $^{27}Al/^{24}Mg$ values in parentheses are secondary ion intensity ratios.

bars may have also formed by diffusional substitution of Mg to Fe in forsterites and spinels. An Fe-bearing fluid may have penetrated into the A1 BO chondrule during aqueous alteration, and/or Fe may have diffused from Fe-Ni sulfide blebs during thermal metamorphism.

It is possible that thermal metamorphism on the parent body caused diffusive redistribution of Mg isotope patterns in chondrules. On the basis of the upper thermal stabilities of the hydrous phases present, thermal metamorphism on the Allende parent body took place at temperatures <673 K (Brearley, 1997), and the duration of metamorphism was estimated to be several million years. Taking the upper limit of self diffusion coefficient of Mg in anorthitic plagioclase estimated by La-Tourrette and Wasserburg (1998) at 673 K (D = 3.0 × 10^{-24} m^2/s), Mg in anorthite can diffuse 10~15 μm within 1 My. Moreover, diffusion may be even faster in mesostasis than in pure anorthite, because it may be less crystalline. Thus thermal metamorphism could have disturbed the Al-Mg system in the A1 compound chondrule.

4.1.2. CDL compound chondrule

The CDL compound chondrule obviously experienced secondary alteration processes in which volatile elements played

an important role (Fig. 4). The Cl and Na zonation (Fig. 4) suggests an influx of Cl and Na after the formation of the entire CDL assemblage.

The Na-rich mesostasis in the PP chondrule, nephelines in the Plg-rich chondrule, ferrous spinels and fayalitic olivines of CDL may have been formed by Fe-alkali-halogen metasomatic alteration. Krot et al. (1995) suggested that heterogeneous aqueous or hydrothermal alteration and subsequent dehydration processes may have produced the alteration features in Allende components. Dark inclusions from Allende also indicate that extensive aqueous alteration and thermal metamorphism may have occurred on the parent body (Kojima and Tomeoka, 1996). Fayalitic olivines and ferrous spinels near the rim of CDL apparently resulted from the penetration of FeO components from the outside after solidification of the whole body of CDL, because olivines and spinels closer to the rim are richer in FeO than those in the inner portion of CDL. Iron may have penetrated through the grain boundaries and cracks which resulted in more fayalitic rims in the PP chondrule. CDL may have reacted with an Fe-rich and ^{16}O-poor fluid as for the A1 chondrule. However, in contrast to the A1 chondrule, CDL apparently also reacted with a Na-Cl-rich fluid. This compositional difference may be due to grain compositions and grain sizes and/or dimensions of fluid conduits responsible for the final product (J. T. Wasson, private communication).

It is possible that the thermal metamorphism caused diffusive redistribution of Mg isotope patterns in the feldspathic mesostasis and plagioclases in CDL. Taking the upper limit of the diffusion coefficient of LaTourrette and Wasserburg (1998) at 673 K, Mg isotopes in the plagioclase can diffuse the distance between the grain boundary and the analyzed point (20~30 μm) within only 1~3 My. The Al-Mg system in feldspathic phases in CDL may have been disturbed by thermal metamorphism.

4.2. Crystallization Process of Chondrules

4.2.1. A1 barred-olivine compound chondrule

The chemical and oxygen isotopic properties strongly suggest that the spinel grain in the A1 BO chondrule crystallized during the chondrule-forming event (Maruyama et al., 1999). Therefore, the formation process of this BO chondrule seems to have been similar to those of ordinary ferromagnesian chondrules. There must have been a difference in the chemical composition of the precursor materials, however.

The enrichment in ^{16}O in some phases in the A1 BO chondrule correlates with the textually inferred crystallization sequence, that is, spinel, olivine and then the mesostasis (Fig. 8). This correlation may result from incomplete O isotopic exchange with nebular gas under rate-limiting processes such as diffusion in melt and/or surface reaction (Maruyama et al., 1999). The O-isotopic composition of the mesostasis rather reflects oxygen isotopic exchange during aqueous alteration and thermal metamorphism on the parent body.

The O isotopic and textural evidence of the A1 BO chondrule suggests that the chondrule was formed by single event such as: (1) Precursor materials were almost totally melted by
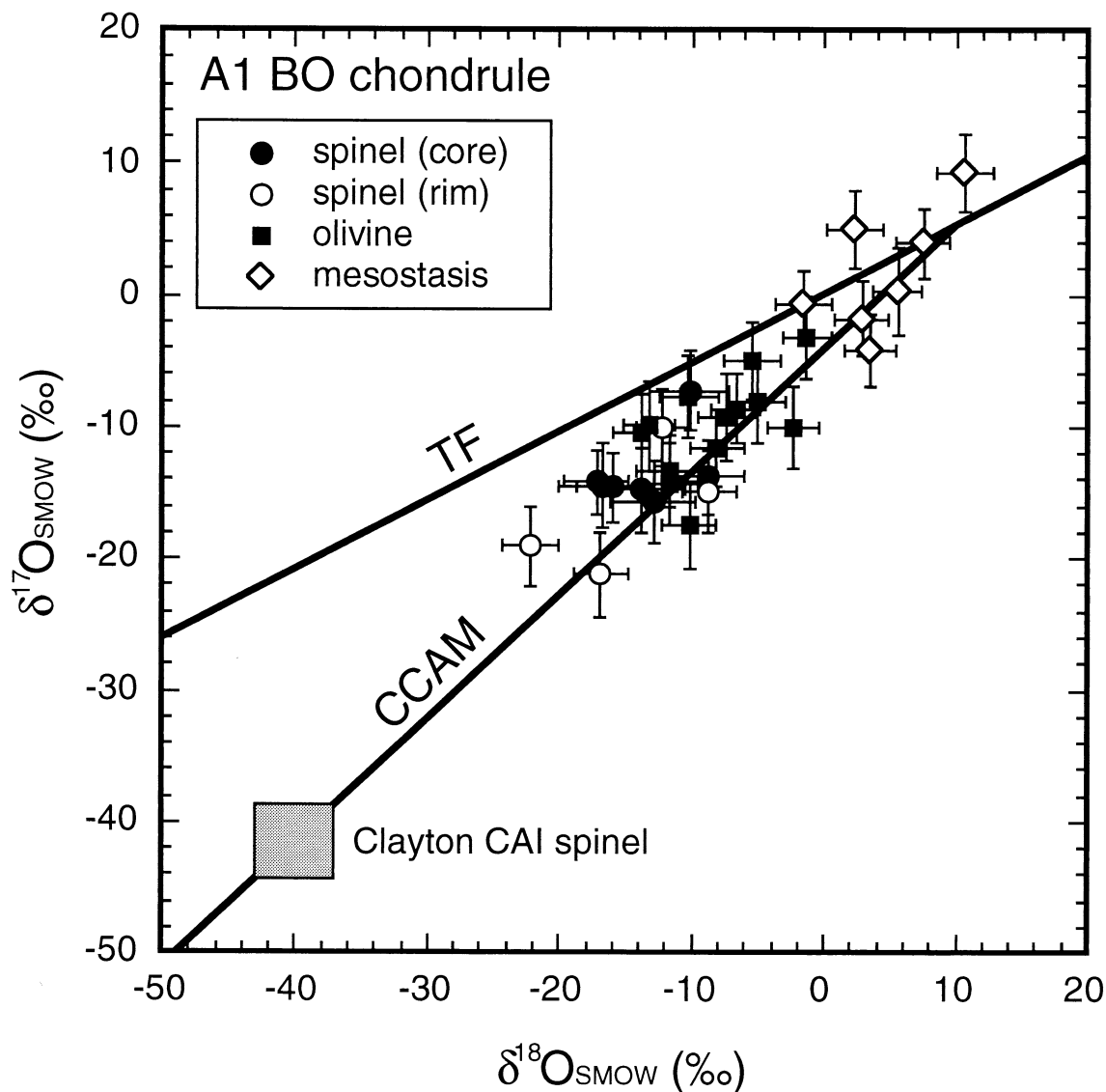
Fig. 8. Oxygen isotopic compositions of minerals in the A1 BO chondrule. The O isotopic composition of the spinel grain is greatly different from that of spinel in CAIs. All errors are $1\sigma_{mean}$. TF: terrestrial fractionation line (Clayton, 1993), CCAM: carbonaceous chondrite anhydrous minerals line (Clayton, 1993). A typical CAI spinel range from Clayton (1993) is also plotted. Ion probe analyses are generally more negative.

a transient heating event. (2) A relatively rapid cooling solidified the melt. The spinel grain crystallized first followed by the olivine. (3) Interstitial melt among barred olivines formed the mesostasis.

4.2.2. CDL compound chondrule

The relict CAI spinel grains in the Plg-rich chondrule were incorporated in chondrule precursors and survived the brief melting event. Because of the sluggish diffusion rate of oxygen in spinel (Reddy and Cooper, 1981), these spinel grains (>6 μm) could not exchange their O-isotopes with the surrounding melt during the chondrule formation event. The higher $\Delta^{17}O$ values may reflect minor overgrowth or beam overlap in the ion probe. On the other hand, the oxygen isotopic compositions of

olivine, pyroxene and plagioclase can be interpreted as the result of an incomplete oxygen isotopic exchange with the nebular gas under rate-limiting processes (Maruyama et al., 1999). Wasson (2000) argued that it was almost certainly impossible to diffuse O into the interior of a static chondrule melt during the brief (1–10 s) period that it was molten. To explain the origin of the O isotopic heterogeneity among minerals in CAIs, Yurimoto et al. (1998) suggested that remelting or metamorphism by reheating events increased the O isotopic exchange between the ambient nebular gas and the newly crystallized minerals in CAIs. The O isotopic variation among the minerals in the Plg-rich chondrule may have resulted from multiple heating processes. A possible energy source for the multiple heating events would be an active protosun as for the
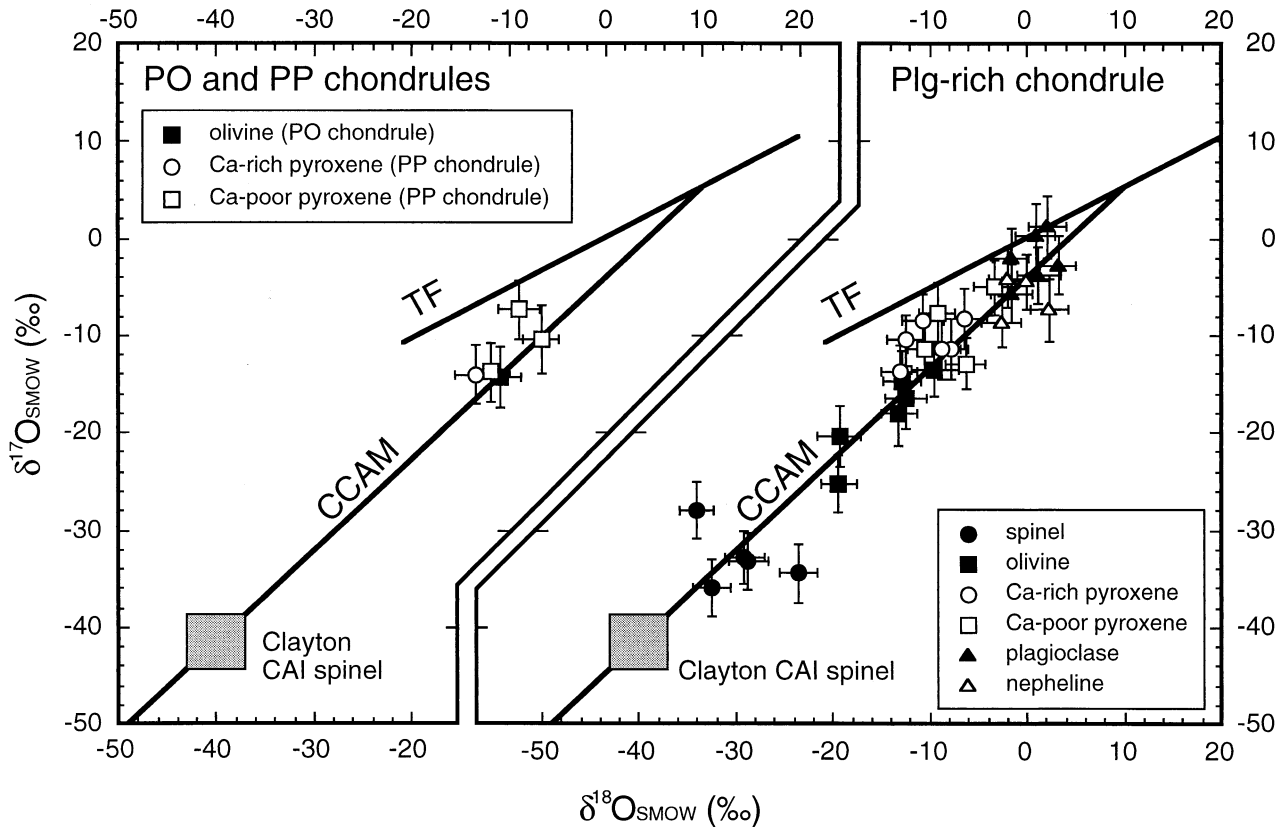
Fig. 9. Oxygen isotopic compositions of minerals in CDL. The O isotopic composition of spinel is close to that of spinel in CAIs. The enrichment of the ^{16}O component among olivine, pyroxene, and plagioclase correlates with the textually inferred crystallization sequence. All errors are $1\sigma_{mean}$. A typical CAI spinel range from Clayton (1993) is also plotted.

X-wind model (Shu et al., 1997). Aqueous alteration may have led to a shift of analytical points of plagioclase closer to $\Delta^{17}O$ = 0‰.

Another characteristic of CDL is that it is a compound chondrule. The textural evidence clearly shows that the formation of the PO chondrule preceded that of the Plg-rich chondrule. However, perhaps because of the large uncertainties, no detectable differences are observed in the ^{26}Al-^{26}Mg systematics.

A plausible scenario for the formation of CDL is the following: (1) The Type-I PO chondrule was formed. This happened by solidification of the molten droplet of low-FeO precursors. (2) The PP chondrule formed around the PO chondrule. The precursors of the PP chondrule were more enriched in Ca than those of the PO chondrule, so that Ca-rich pyroxenes dominate the PP chondrule. (3) The Ca-Al-rich molten droplet (i.e., the Plg-rich chondrule) encountered the PO-PP compound chondrule, or the PO-PP chondrule incorporated into a mix of CAI materials and Na-rich nebular materials. The molten droplet was incompletely melted, and CAI spinels were incorporated as precursors and survived melting during the transient heating event. Spinel is a more refractory mineral than the other chondrule-forming minerals (e.g., olivine and pyroxene), therefore spinels in the Plg-rich chondrule could have been a relict phase if the heating period was brief and/or the heating temperature was relatively lower. The spinel grains in the Plg-rich chondrule were partly melted by the surrounding melt.

Therefore, the peak temperature of the formation of the Plg-rich chondrule may have been slightly higher than the melting point of spinel. (4) The solidification of the Ca-Al-rich molten droplet. The solidification of the Plg-rich chondrule was completed in this stage.

The chemical compositions of the PO, the PP, and the Plg-rich chondrules are quite different from each other. Therefore, precursors for each part of CDL must have been different to each other. This shows that dust aggregates of chondrule precursors were chemically heterogeneous in the protoplanetary disk.

5. CONCLUSIONS

Two spinel-bearing compound chondrules from the Allende CV chondrite were investigated. Their petrological properties, oxygen isotopic compositions and Al-Mg isotopic compositions were determined to clarify the relationship between chondrules and CAIs.

The oxygen isotopic composition of the spinel grain in the A1 BO chondrule ($\Delta^{17}O$ = -7.1 ± 0.9‰) is essentially equal to those of coexisting olivines ($\Delta^{17}O$ = -5.6 ± 0.8‰), but is much ^{16}O-poorer than spinels in CAIs. It apparently crystallized first during the formation of the A1 BO chondrule. On the other hand, the strongly serrated character of the spinel grains in the Plg-rich chondrule of CDL can be explained by reaction with a spinel-undersaturated liquid. The oxygen isotopic compositions of the
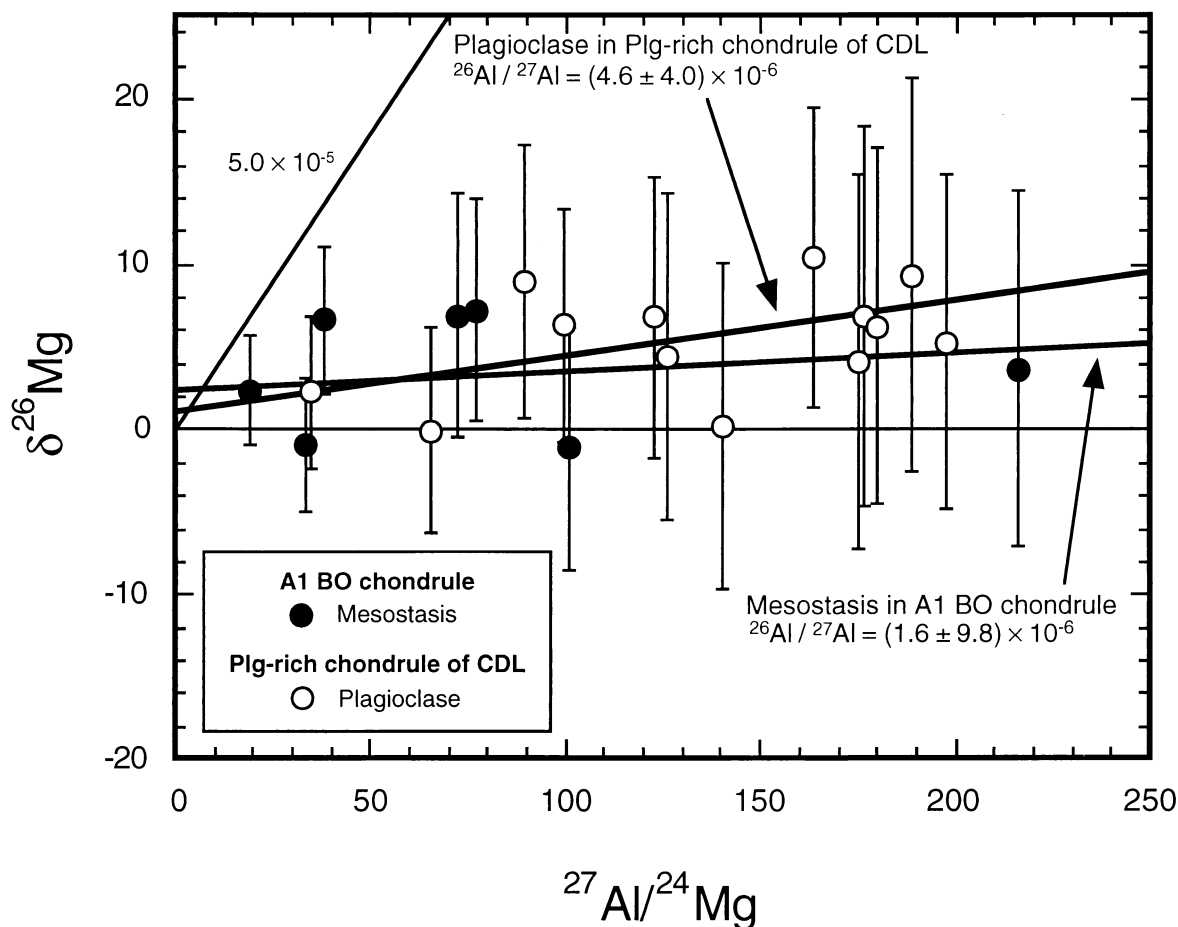
Fig. 10. $\delta^{26}Mg$ vs. $^{27}Al/^{24}Mg$ for the feldspathic mesostasis in the A1 BO chondrule and plagioclase in the Plg-rich chondrule of CDL. The isochron of the feldspathic mesostasis in the A1 BO chondrule may have been disturbed by aqueous alteration and thermal metamorphism. A correlation line for the data of plagioclase in the Plg-rich chondrule is also shown. Plagioclase shows slight $^{26}Mg^*$. All errors are $2\sigma_{mean}$. A reference line is shown corresponding to an initial $^{26}Al/^{27}Al$ ratio of 5.0×10^{-5}.

spinel grains in the Plg-rich chondrule ($\Delta^{17}O = -17.3\pm2.0‰$) are only ~5‰ greater than those of spinels in CAIs. Moreover, the oxygen isotopic compositions of olivine ($\Delta^{17}O = -10.4\pm1.0‰$) and pyroxene ($\Delta^{17}O_{CPx+OPx} = -5.4\pm0.7‰$) in the Plg-rich chondrule are quite different from that of spinel. Therefore, the spinel grains in the Plg-rich chondrule are obviously relict phases that survived the chondrule-forming event; these relict spinel grains probably originated in coarse-grained CAIs. The oxygen isotopic compositions of olivine, pyroxene and plagioclase can be interpreted as the result of an incomplete oxygen isotopic exchange with nebular gas under rate-limiting processes.

Most likely aqueous alteration and thermal metamorphism on the parent body led to disturbed oxygen and Al-Mg isotopic compositions of the chondrule constituents. The CDL compound chondrule contains the Fe-alkali-halogen metasomatic alteration products. Although the mesostasis of the A1 BO chondrule is Na-Cl-free, the disturbed ^{26}Al-^{26}Mg isochron in the mesostasis supports the idea of alteration on the Allende parent body. The alteration products in CDL ($\Delta^{17}O_{Nepheline} = -5.7\pm1.3‰$) are considerably richer in ^{16}O than that in the A1 BO chondrule ($\Delta^{17}O_{Mesostasis} = -0.6\pm1.4‰$). This suggests

that the fluids which reacted with Allende chondrules were not only chemically but also isotopically heterogeneous.

The petrological and isotopical properties of individual minerals in the compound Al-rich chondrules suggest that ^{16}O-poor gas in the solar nebula was preserved in the chondrule forming region and relatively ^{16}O-rich chondrule precursors in the gas gradually changed to ^{16}O-poor through multi-heating events.

Associate editor: U. Ott

REFERENCES

Bischoff A. and Keil K. (1984) Al-rich objects in ordinary chondrites: Related origin of carbonaceous and ordinary chondrites and their constituents. *Geochim. Cosmochim. Acta* **48,** 693–709.

Brearley A. J. (1997) Disordered biopyriboles, amphibole, and talc in the Allende meteorite: Products of nebular or parent body aqueous alteration? *Science* **276**, 1103–1105.

Brigham C. A. (1990) Isotopic heterogeneity in calcium-aluminum rich meteoritic inclusions. Ph.D. thesis, California Institute of Technology.

Catanzaro E. J., Murphy T. J., Garner E. L., and Shields W. R. (1966) Absolute isotopic abundance ratios and atomic weight of magnesium. *J. Res. Natl. Bur. Stand.* **70A**, 453–458.

Choi B.-G., McKeegan K. D., Leshin L. A., and Wasson J. T. (1997) Origin of magnetite in oxidized CV chondrites: In situ measurement of oxygen isotope compositions of Allende magnetite and olivine. *Earth Planet. Sci. Lett.* **146**, 337–349.

Clayton R. N. (1993) Oxygen isotopes in meteorites. *Annu. Rev. Earth Planet. Sci.* **21**, 115–149.

Clayton R. N., Onuma N., Grossman L., and Mayeda T. K. (1977) Distribution of the pre-solar component in Allende and other carbonaceous chondrites. *Earth Planet. Sci. Lett.* **34**, 209–224.

Clayton R. N., Onuma N., Ikeda Y., Mayeda T. K., Hutcheon I. D., Olsen E. J., and Molini-Velsko C. (1983) Oxygen isotopic compositions of chondrules in Allende and ordinary chondrites. In *Chondrules and Their Origins* (ed. E. A. King), pp. 37–43, Lunar and Planetary Institute, Houston, Texas.

Gooding J. L. and Keil K. (1981) Relative abundances of chondrule primary textural types in ordinary chondrites and their bearing on conditions of chondrule formation. *Meteoritics* **16**, 17–43.

Grossman J. N. (1988) Formation of chondrules. In *Meteorites and the Early Solar System* (eds. J. F. Kerridge and M. S. Matthews), pp. 680–696, Univ. of Arizona Press, Tucson, Arizona.

Hervig R. L. and Steele I. M. (1992) Oxygen isotopic analysis of Allende olivine by ion microprobe and implications for chondrule origin. *Lunar Planet. Sci. Conf. XXIII* 525–526(abstr.).

Hiyagon H. (1997) *In situ* analysis of oxygen isotopes and Fe/Mg ratios in olivine using SIMS: Preliminary results for an Allende chondrule. *Antarct. Meteorite Res.* **10**, 249–274.

Hutcheon I. D. and Jones R. H. (1995) The ^{26}Al-^{26}Mg record of chondrules: Clues to nebular chronology. *Lunar Planet. Sci. Conf. XXVI* 647–648 (abstr.).

Ikeda Y. and Kimura M. (1995) Anhydrous alteration of Allende chondrules in the solar nebula I: Description and alteration of chondrules with known oxygen-isotopic compositions. *Proc. NIPR Symp. Antarct. Meteorites* **8**, 97–122.

Kim G. L., Yurimoto H., and Sueno S. (1998) ^{16}O-enriched melilite and anorthite coexisting with ^{16}O-depleted melilite in a CAI. *Lunar Planet. Sci. Conf. XXIX* #1344 (abstr.).

Kim G. L., Yurimoto H., and Sueno S. (2002) Oxygen isotopic composition of a compound Ca-Al-rich inclusion from Allende meteorite: Implications for origin of palisade bodies and O-isotopic environment in the CAI forming region. *J. Min. Petrol. Sci.* **97**, 161–167.

Koike O., Yurimoto H., Nagasawa H., and Sueno S. (1993) Ion microprobe measurements of Mg isotopes in Type B1 CAI of Allende meteorite. *Proc. NIPR Symp. Antarct. Meteorites* **6**, 357–363.

Kojima T. and Tomeoka K. (1996) Indicators of aqueous alteration and thermal metamorphism on the CV parent body: Microtextures of a dark inclusion from Allende. *Geochim. Cosmochim. Acta* **60**, 2651–2666.

Krot A. N. and Keil K. (2002) Anorthite-rich chondrules in CR and CH carbonaceous chondrites: Genetic link between calcium-aluminum-rich inclusions and ferromagnesian chondrules. *Meteoritics Planet. Sci.* **37**, 91–111.

Krot A. N. and Wasson J. T. (1995) Igneous rims on low-FeO and high-FeO chondrules in ordinary chondrites. *Geochim. Cosmochim. Acta* **59**, 4951–4966.

Krot A. N., Scott E. R. D., and Zolensky M. E. (1995) Mineralogical and chemical modification of components in CV3 chondrites: Nebular or asteroidal processing? *Meteoritics* **30**, 748–775.

Krot A. N., Hutcheon I. D., and Keil K. (2002) Plagioclase-rich chondrules in the reduced CV chondrites: Evidence for complex formation history and genetic links between calcium-aluminum-rich inclusions and ferromagnesian chondrules. *Meteoritics Planet. Sci.* **37**, 155–182.

LaTourrette T. and Wasserburg G. J. (1998) Mg diffusion in anorthite: Implications for the formation of early solar system planetesimals. *Earth Planet. Sci. Lett.* **158**, 91–108.

Lee T., Papanastassiou D. A., and Wasserburg G. J. (1977) Aluminum-26 in the early solar system: Fossil or fuel? *Astrophys. J.* **211**, L107–L110.

Lux G., Keil K., and Taylor G. J. (1981) Chondrules in H3 chondrites: Textures, compositions and origins. *Geochim. Cosmochim. Acta* **45**, 675–685.

MacPherson G. J., Davis A. M., and Zinner E. K. (1995) The distribution of aluminum-26 in the early Solar System – A reappraisal. *Meteoritics* **30**, 365–386.

Maruyama S., Yurimoto H., and Sueno S. (1999) Oxygen isotope evidence regarding the formation of spinel-bearing chondrules. *Earth Planet. Sci. Lett.* **169**, 165–171.

Mason B. and Martin P. M. (1977) Geochemical differences among components of the Allende meteorite. *Smithsonian Contrib. Earth Sci.* **19**, 84–95.

McSween H. Y. (1977) Chemical and petrographic constraints on the origin of chondrules and inclusions in carbonaceous chondrites. *Geochim. Cosmochim. Acta* **41**, 1843–1860.

Misawa K. and Fujita T. (1994) A relict refractory inclusion in a ferromagnesian chondrule from the Allende meteorite. *Nature* **368**, 723–726.

Misawa K. and Nakamura N. (1988) Highly fractionated rare-earth elements in ferromagnesian chondrules from the Felix (CO3) meteorite. *Nature* **334**, 47–50.

Reddy K. P. R. and Cooper A. R. (1981) Oxygen diffusion in magnesium aluminate spinel. *J. Am. Ceram. Soc.* **64**, 368–371.

Rubin A. E. (1994) Fragments of history preserved. *Nature* **368**, 691.

Russell S. S., Srinivasan G., Huss G. R., Wasserburg G. J., and MacPherson G. J. (1996) Evidence for widespread ^{26}Al in the solar nebula and constraints for nebula time scales. *Science* **273**, 757–762.

Russell S. S., MacPherson G. J., Leshin L. A., and McKeegan K. D. (2000) ^{16}O enrichments in aluminum-rich chondrules from ordinary chondrites. *Earth Planet. Sci. Lett.* **184**, 57–74.

Sheng Y. J., Hutcheon I. D., and Wasserburg G. J. (1991) Origin of plagioclase-olivine inclusions in carbonaceous chondrites. *Geochim. Cosmochim. Acta* **55**, 581–599.

Shu F. H., Shang H., Glassgold A. E., and Lee T. (1997) X-rays and fluctuating x-winds from protostars. *Science* **277**, 1475–1479.

Wark D. A. and Lovering J. F. (1982) Evolution of Ca-Al-rich bodies in the earliest solar system: Growth by incorporation. *Geochim. Cosmochim. Acta* **46**, 2595–2607.

Wasson J. T. (1993) Constraints on chondrule origins. *Meteoritics* **28**, 14–28.

Wasson J. T. (2000) Oxygen-isotopic evolution of the solar nebula. *Rev. Geophys.* **38**, 491–512.

Wasson J. T., Krot A. N., Lee M. S., and Rubin A. E. (1995) Compound chondrules. *Geochim. Cosmochim. Acta* **59**, 1847–1869.

Weinbruch S., Zinner E. K., El Goresy A., Steele I. M., and Palme H. (1993) Oxygen isotopic composition of individual olivine grains from the Allende meteorite. *Geochim. Cosmochim. Acta* **57**, 2649–2661.

Wood J. A. (1996a) Unresolved issues in the formation of chondrules and chondrites. In *Chondrules and the Protoplanetary Disk* (eds. R. H. Hewins, R. H. Jones, and E. R. D. Scott), pp. 55–69, Cambridge Univ. Press, Cambridge, UK.

Wood J. A. (1996b) Processing of chondritic and planetary material in spiral density waves in the nebula. *Meteoritics Planet. Sci.* **31**, 641–645.

Yurimoto H., Ito M., and Nagasawa H. (1998) Oxygen isotope exchange between refractory inclusion in Allende and solar nebula gas. *Science* **282**, 1874–1877.